56-26
N91-70704
P-20

KSC-NASA/ UCF COOPERATIVE AGREEMENT

MATERIALS PERFORMANCE RESEARCH PROGRAM

END OF THE FIRST YEAR STATUS REPORT

January-December,1990

Submitted by: Dr. V. H. Desai, P.I.
Mr. Kirk Scammon
Mr. Edward Principe
Ms. Lisa Sperling

Mechanical & Aerospace Engineering Department
College of Engineering
University of Central Florida

EXECUTIVE SUMMARY:

Nearly 40% of the materials related failures at Kennedy space center are corrosion related. Half of these are estimated to be stress corrosion cracking (SCC) failures. Prevalence of acidic chloride environment and a broad range of service conditions make the situation severe and complex for variety of materials that are expected to perform well.

During the first year of this research program, nine Fe and Ni based alloys were rated for SCC susceptibility by slow strain rate testing (SSR). Progress was made in determine fundamental SCC parameters such as crack propagation rate, activation energy, incubation or initiation time and threshold stress intensity through the use of innovative techniques such as lead pulsing, laser holography, and interferometry. These studies will lead to service life prediction. Also, hydrogen embrittlement susceptibility study of highly corrosion resistant Ni based alloys has initiated. The alloys being tested are candidate materials for hydrogen storage tanks. An electrochemical system for hydrogen permeation study has been setup and tested while embrittlement studies through SSR technique have initiated.

Two additional projects were identified for the second year of research. These are characterization of acidified sea water used to simulate KSC environment and study of concrete corrosion and prevention.

BACKGROUND:

Corrosion accounts for about 40% of the materials related failures encountered at NASA's Kennedy Space Center. Nearly half such failures are due to stress corrosion cracking (SCC), making it the most significant cause of material failure. SCC is followed by pitting, hydrogen embrittlement, uniform corrosion, galvanic corrosion, and exfoliation in its order of severity. This is graphically represented in figures 1 and 2. The variety of service conditions and metallic alloys employed make the situation complex requiring a concentrated effort to find failure mechanisms and provide solutions through greater understanding. Vicinity of sea water and presence of HCl acid mist following SRB blast make the corrosion conditions very severe. For example, the hydrogen storage tanks undergo almost round the year maintenance. This has lead to the suggestion of using highly corrosion resistant Ni base alloys as materials of construction for these tanks. Table I summarizes the environment handled and the variety of metallic alloys used at KSC.

MATERIALS RELATED FAILURES

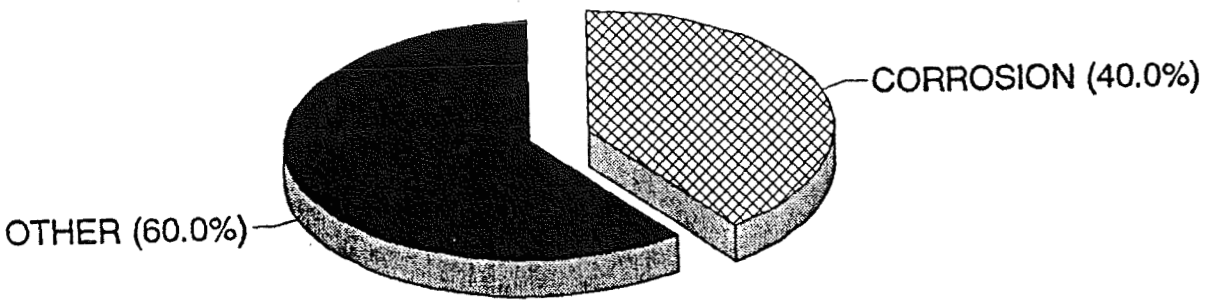

Figure 1

CORROSION RELATED FAILURES

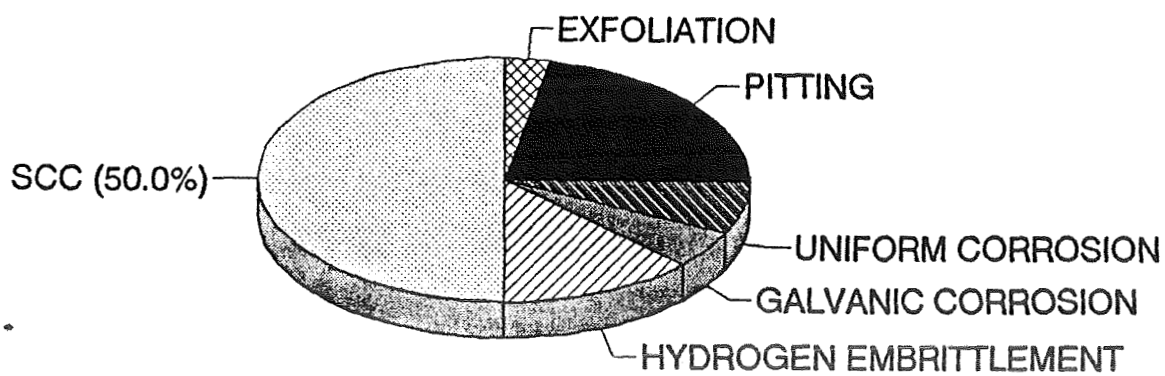

Figure 2

Complexity of KSC Situation

Environment Handled	Metallic Alloy Used
Marine	1,2,3,4,5,6
Marine + HCl acid mist	1,2,3,4,5
Gaseous Nitrogen	1,2,3,4
Gaseous Helium	1,2,3,4
Liquid and Gaseous Oxygen	1,4
Liquid Hydrogen	1,4
Gaseous Hydrogen	1,2,4
Liquid Nitrogen	1,4
Monomethyl Hydrazine (MMH)	1
Hydrazine (N_2H_4)	1
Nitrogen Tetroxide (N_2O_4)	1

Key: Metallic Alloys

1	Stainless Steels
2	C Steels and Alloy Steels
3	Quenched and Tempered Steels
4	High Nickel Alloys
5	Aluminum Alloys
6	Titanium Alloys

Table I

OBJECTIVES:

Task I — Determine the SCC susceptibility of various Fe and Ni base alloys by slow strain rate (SSR) tests in simulated laboratory environment (sea water acidified to pH 1) and rate these alloys in order of their performance for use at or in the vicinity of launch complex.

Task II — SCC studies through innovative techniques

(A) Using load pulsing method, determine the velocity of crack propagation and activation energy for both trans and intergranular mode of cracking of austenitic stainless steels in chloride environments. Also, determine the effects of temperature, environment and metallurgical variables on SCC susceptibility and relate to service life predictions and protection.

(B) Using coherent optical techniques such as laser holography and speckle photography determine the time to initiate SCC, threshold stress intensity and crack propagation rate. Relate this data to service life predictions and develop the technique to quickly assess the effect of metallurgical variables on SCC parameters.

Task III — Hydrogen susceptibility studies

Determine the susceptibility to hydrogen damage of highly corrosion resistant alloys such as Hastelloys C22, C276, G30, Inconel 625, and Inconel 718. And recommend alloys resistance to hydrogen storage tanks (3,000 to 6,000 psi) which can give at least ten years of trouble free service.

Task I SCC SUSCEPTIBILITY STUDIES BY SSR TESTS

Approach

1. Flat plate specimens of various alloys were pulled in air and acidified sea water at strain rate of ~ 10-6 per second.

2. The susceptibility to SCC was evaluated by comparing the air and sea water tests. Six criteria were used to determine susceptibility namely time to failure, maximum stress, strain at maximum stress, maximum strain, % reduction in area and fracture area ratio (FAR).

3. In order to assess the effect of strain rate, three different strain rates were utilized for studying the susceptibility of three alloys.

Progress

1. Nine alloys have been assessed for SCC susceptibility. The results of these tests are summarized in Table II. Each data point is an average of three tests and indicates % decrease in the value of respective parameter compared with the test in air.

2. Based on the six parameters listed earlier, the alloys are rated as follows:

   Highly susceptible to SCC
   - 303 steel (annealed)
   - 17-4 PH steel (H 1025)
   - 17-4 PH steel (H 900)

   Moderately susceptible to SCC
   - 316 L steel (annealed)
   - 304 steel (annealed)
   - 17-4 PH steel (annealed)
   - 17-4 PH steel (H 1150)

   Non-susceptible to SCC
   - Inconel 718 (annealed)
   - Inconel 718 (40 HRC)

3. The three alloys tested to assess the effect of strain rate indicated a great dependance of susceptibility on the strain rate chosen to run SSR tests.

ALLOY	TIME TO FAILURE	MAXIMUM STRESS	STRAIN AT MAXSTRESS	MAXIMUM STRAIN	REDUCTION IN AREA
303 ANNEALED	-71%	-34%	-75%	-68%	-75%
304L ANNEALED	NO CHANGE	NO CHANGE	-4%	-6%	-16%
316L ANNEALED	NO CHANGE	NO CHANGE	-12%	-12%	NO CHANGE
INCONEL 718	NO CHANGE	NO CHANGE	NO CHANGE	NO CHANGE	NO CHANGE
IN 718 40 HRC	NO CHANGE	NO CHANGE	NO CHANGE	NO CHANGE	NO CHANGE
17-4PH ANNEALED	-10%	NO CHANGE	NO CHANGE	NO CHANGE	-17%
17-4PH H1150	-5%	NO CHANGE	-9%	-9%	-8%
17-4PH H1025	-42%	NO CHANGE	-40%	-60%	-67%
17-4PH H900	-30%	NO CHANGE	NO CHANGE	-40%	-27%

TABLE # 2 DIFFERENCE BETWEEN AIR AND SOLUTION TESTS

4. We recommend the following practice in SCC investigation through SSR tests.

Recommended Practice for SCC Investigation by SSR Tests

1. Perform SSR experiments on each of the 50 different alloys at approx. 10^{-6} per sec. strain rate in acidified (pH 1) sea water.

2. Discard alloys that are highly susceptible as determined by a combination of ultimate strength, time to failure, reduction in area, % elongation, strain to fracture and strain at maximum stress.

3. Run additional SSR experiments on moderately susceptible and non-susceptible alloys at strain rates of 10^{-5} and 10^{-7} per sec.

4. Alloys that do not show susceptibility at any of the three strain rates are not susceptible to SCC.

5. Subject all other alloys to SEM fractographic investigation, determine FAR and rank them in order using all the available data.

Task IIA SCC STUDIES THROUGH LOAD PULSING METHOD

Approach

1. Cylindrical specimens of 316 stainless steel were subjected to periodic impulse load of about 5% over the base load which was typically maintained at about 80% yield strength of the alloy. This load pulsing was carried out while the specimens were subjected to a 5% by weight LiCl environment.

2. Tests are being conducted in the range of 110° to 170°C in a autoclave so that different test temperatures could be achieved and maintained while keeping the chloride concentration constant.

3. The crack tip blunting obtained on the fractured surface due to pulsed loading was observed under scanning electron microscope (SEM) as parallel markings. A micrograph indicating such marking in trans and intergranular areas of fracture is shown in figure 3.

4. The average distance between markings when divided by the time interval between pulsing events yields crack propagation rate.

5. A plot of velocity of crack propagation versus test temperature (Arrhenius plot) gives the activation energy required for the propagation of crack.

Progress

1. Tests have been conducted on 316 stainless steel specimens in LiCl environment at 110° and 170° in an autoclave.

2. Problems encountered in "swagelok" fittings and leaking from blow-off valve of the autoclave have been corrected.

3. SEM observations have been carried out on the fractured surface and crack propagation rates for TSCC and ISCC modes of cracking have been deduced. Table III summarizes these results. Each data is an average of several observations.

4. A preliminary Arrhenius type of plot is shown in figure 4 for TSCC. It is too early to calculate activation energy and predict the mechanism of SCC. More data at several other temperatures is awaited.

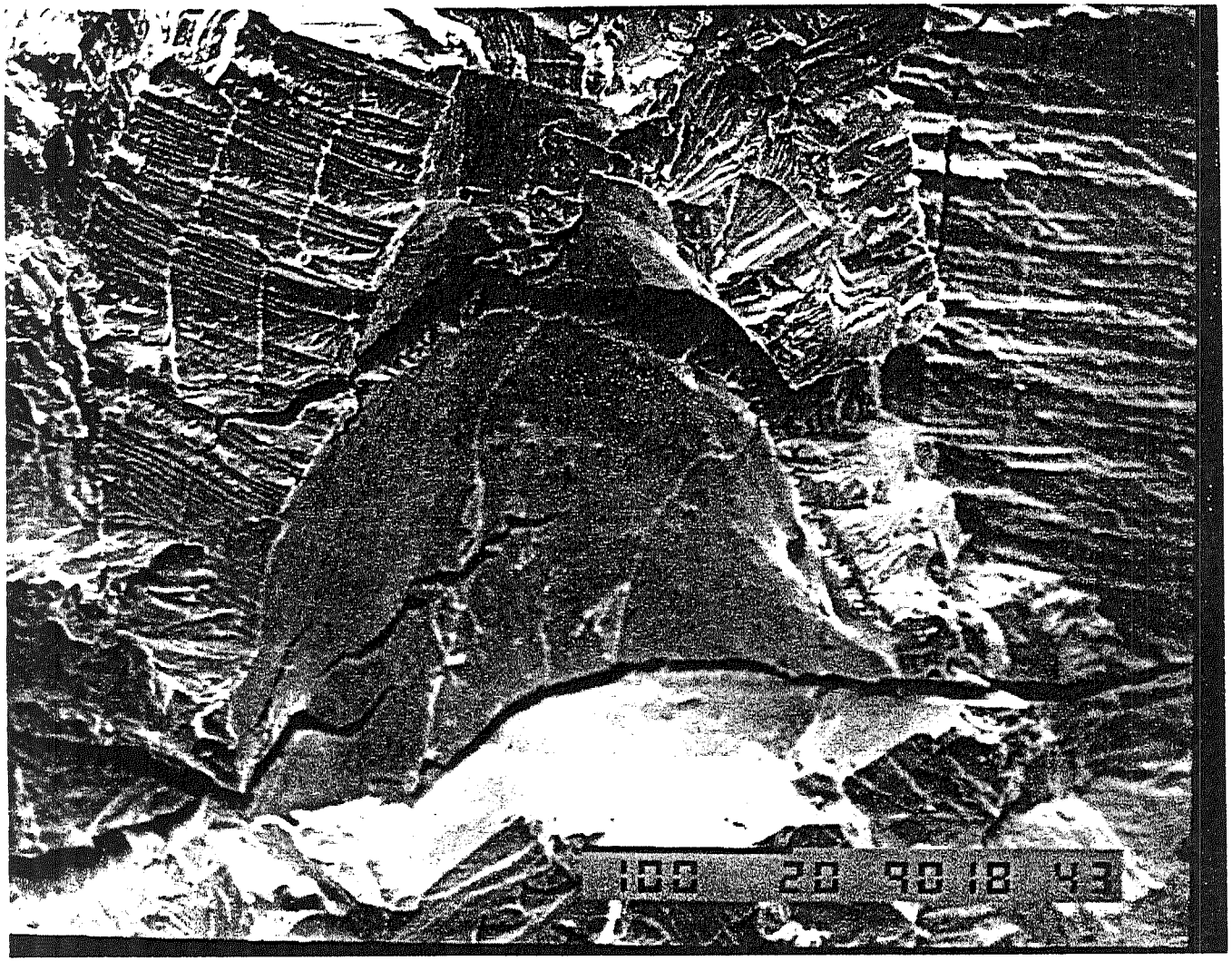

Figure 3 Crack front marking on trans and intergranular fracture

ORIGINAL PAGE IS
OF POOR QUALITY

ISCC Velocity = 2 to 3 x (TSCC Velocity)

TEMP.	VELOCITY (10^-7 m/s)	
	TSCC	ISCC
170 C	2.117	4.423
130 C	1.390	4.550

Table III

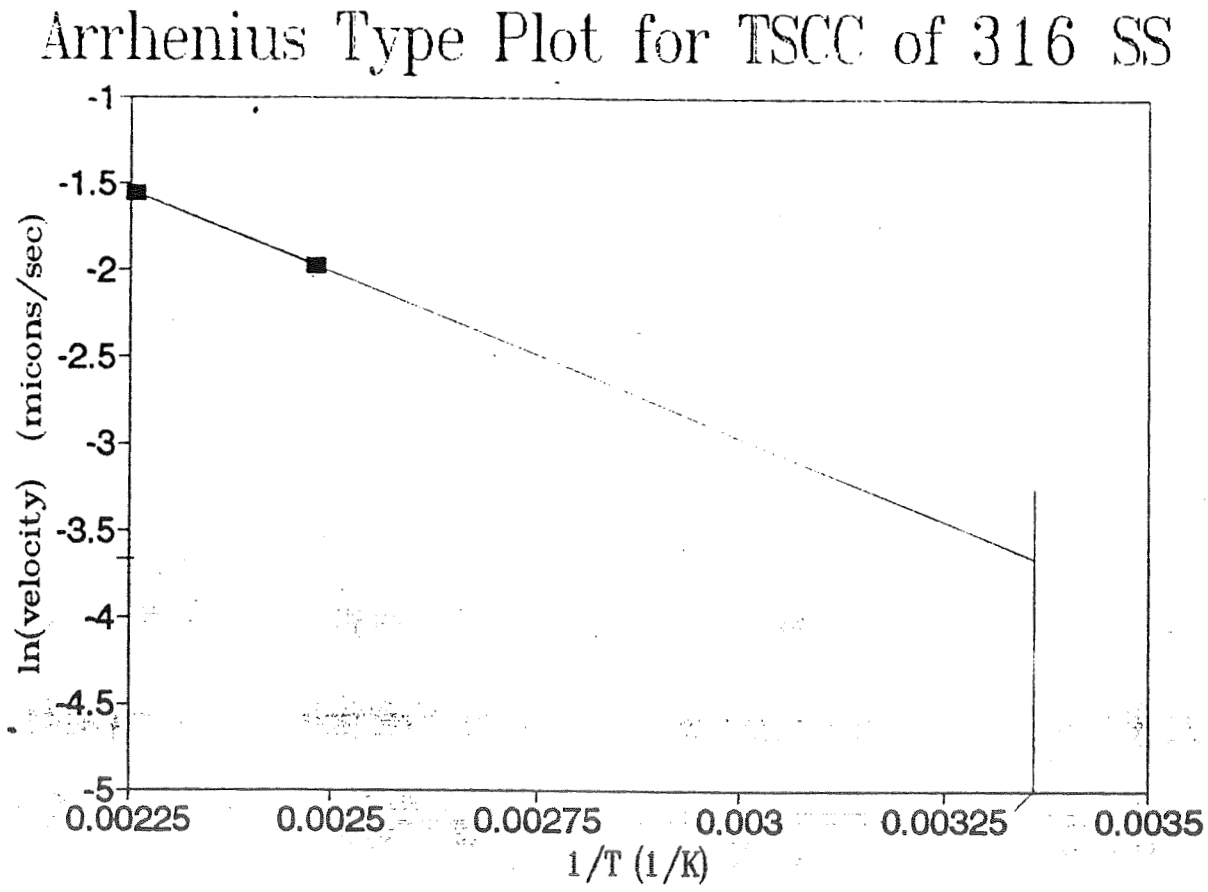

Figure 4

Task II B SCC STUDIES THROUGH LASER HOLOGRAPHY AND SPECKLE INTERFEROMETRY.

Approach

1. Double cantilever beam (DCB) Cu-30Zn brass (as shown in figure 5) are wedge loaded in 15N ammoniacal solution and placed on optical table.

2. The SCC initiation, propagation and arrest are monitored in the schematic shown in figure 6.

Progress

1. Chosen alloy and specimen geometry was shown to crack easily at room temperature in ammoniacal solution with short initiation time and appreciable propagation rate to allow real-time holography.

2. Real-time holography is demonstrated to be successful in determining SCC initiation time. Figure 7 shows a typical holograph with fringe patterns surrounding the crack tip. In many alloys initiation time is the predominant parameter which governs the extent of SCC susceptibility.

3. Local displacements due to SCC have been successfully measured. Finite element model has been developed to verify measured displacement data and determine stress field. A typical result is represented in figure 8.

4. The experimental procedure to evaluate K_{ISCC} is being finalized.

5. Work is continuing to measure SCC crack velocity by speckle photography.

6. A modified specimen geometry and experimental set up is developed for speckle photography as shown in figures 9 and 10.

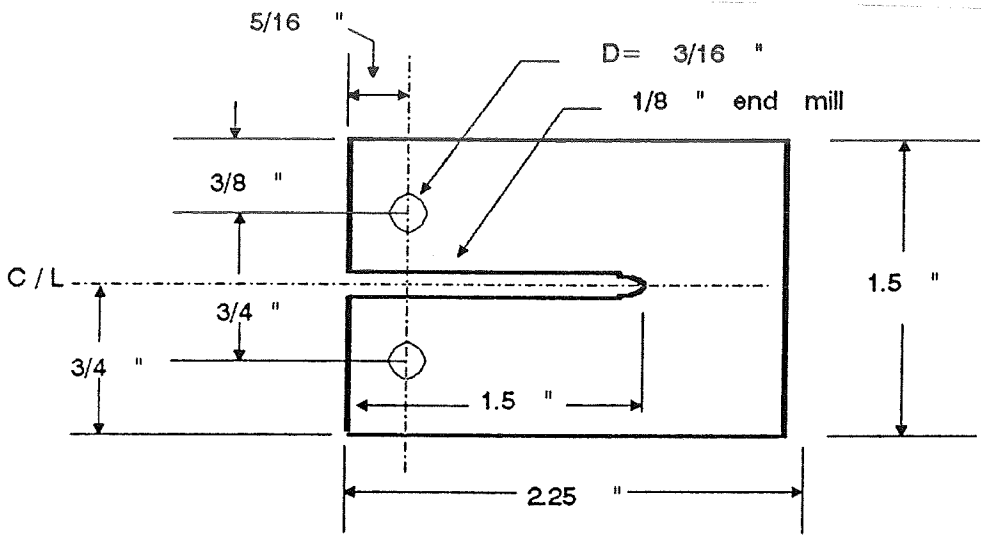

Figure 5 DCB specimen geometry

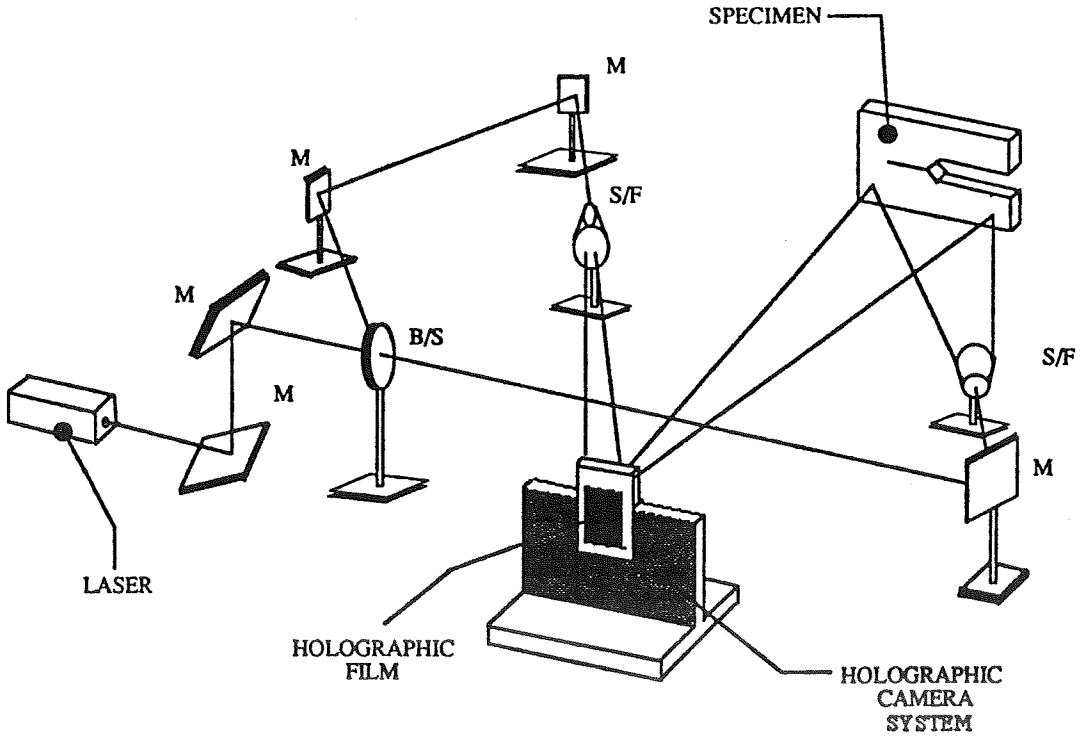

Figure 6 Coherent optics test setup

ORIGINAL PAGE IS
OF POOR QUALITY

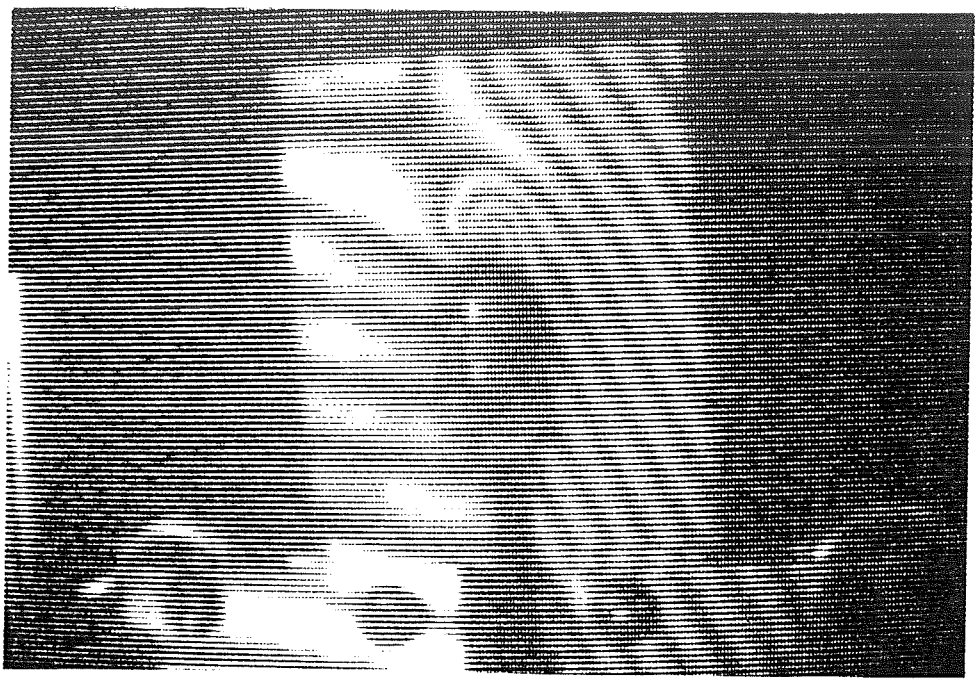

Figure 7 Holograph with fringe patterns surrounding crack tip

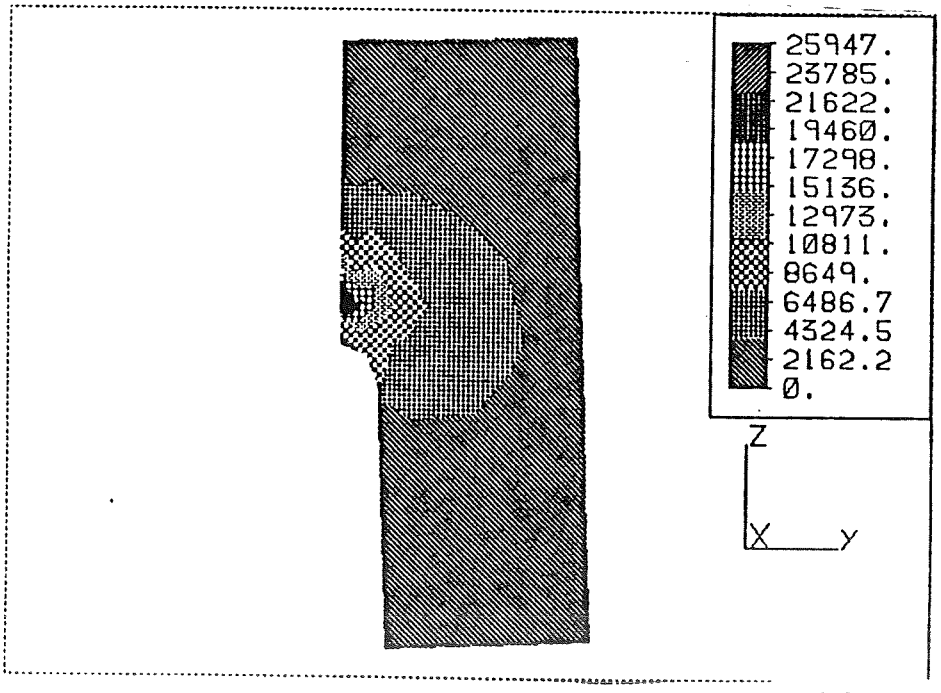

Figure 8 Stress field calculation

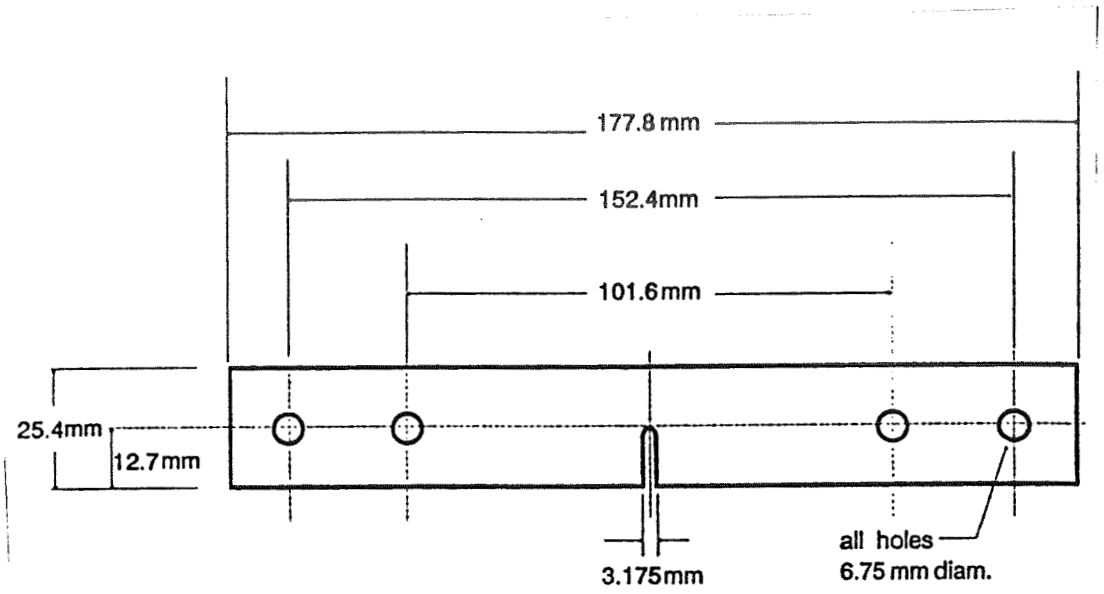

Figure 9 Modified specimen geometry

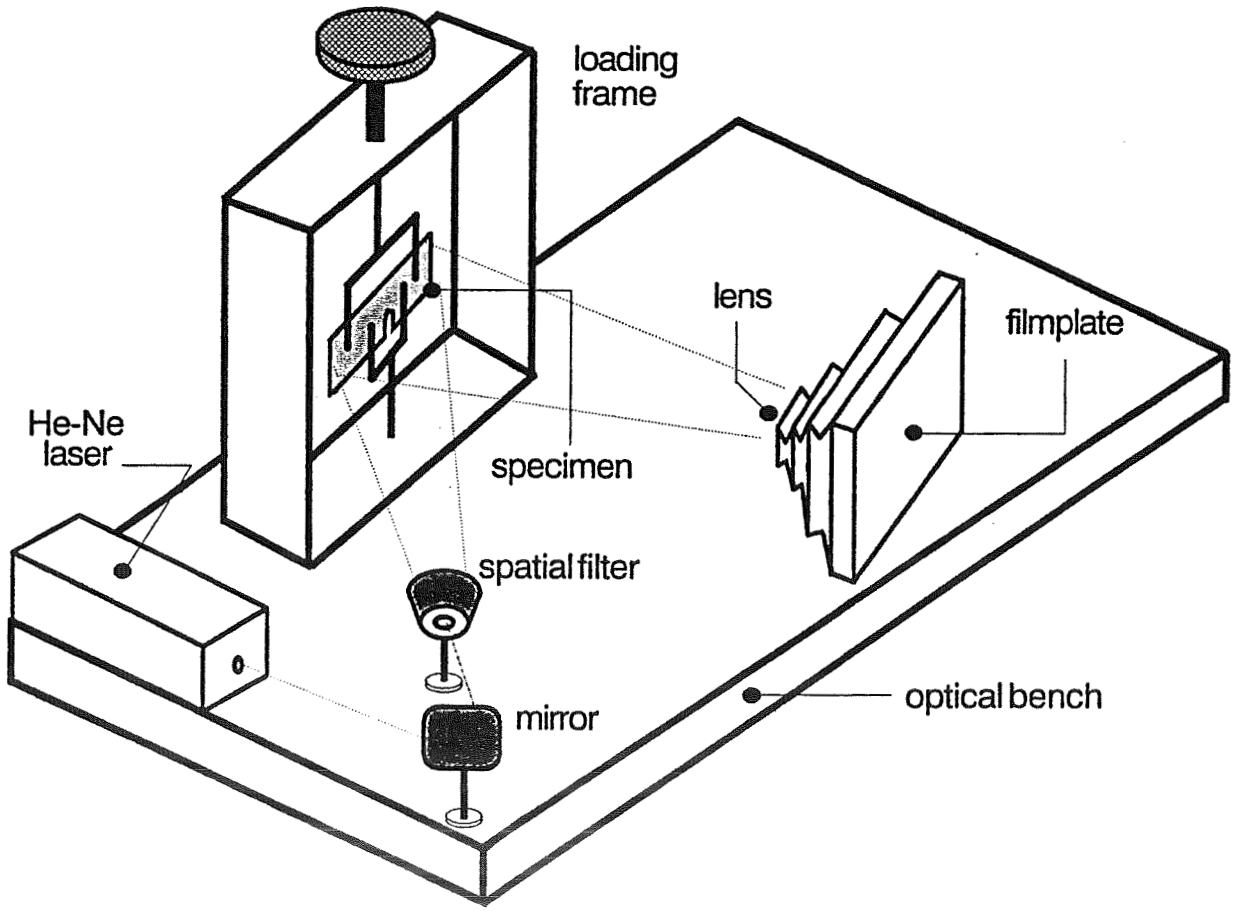

Figure 10 Test setup for speckle photography

Task III. HYDROGEN SUSCEPTIBILITY STUDIES.

Approach

1. This study is divided into two tasks. The first task is to measure coefficient of diffusion of hydrogen in Hastelloys C-22, C-276, G30 and Inconels 625 and 718.

2. The diffusivity is measured using Devanathan-Stacharsky method in which hydrogen in cathodically charged on one side of the thin foil specimen and is oxidized on the other side as it diffuses through. The steady state permeation current is related to diffusivity by one of the several mathematical techniques. This experimental setup is shown in figure 11.

3. The second task is to assess the hydrogen embrittlement susceptibility of the above mentioned materials. This will be accomplished by cathodically charging cylindrical tensile test-type specimens to hydrogen saturation followed by SSR tests.

4. The hydrogen susceptibility will be determined by the loss of strength, loss of ductility and fractographic evaluation.

5. The fractographic evaluation will include determination of fracture area ratio (FAR), dimple size ratio (R), and scanning auger microscopy (SAM) to study effect of cold working and aging on grain boundary precipitation or impurity segregation.

Progress

1. Thin foil specimens for H permeation studies and cylindrical specimens for H embrittlement studies have been procured or fabricated for all the alloys listed above.

2. Established the methodology of H permeation tests. Verified the operation and performance of the permeation cell by testing annealed iron. Iron has a very high diffusivity even at room temperature with D = 2.7 X 10^{-6} cm^2/s. The permeation record for annealed Fe is shown in figure 12. Table IV shows the values of diffusion coefficient obtained by three different analysis. They all seem to be in reasonable agreement with the expected value of H diffusivity.

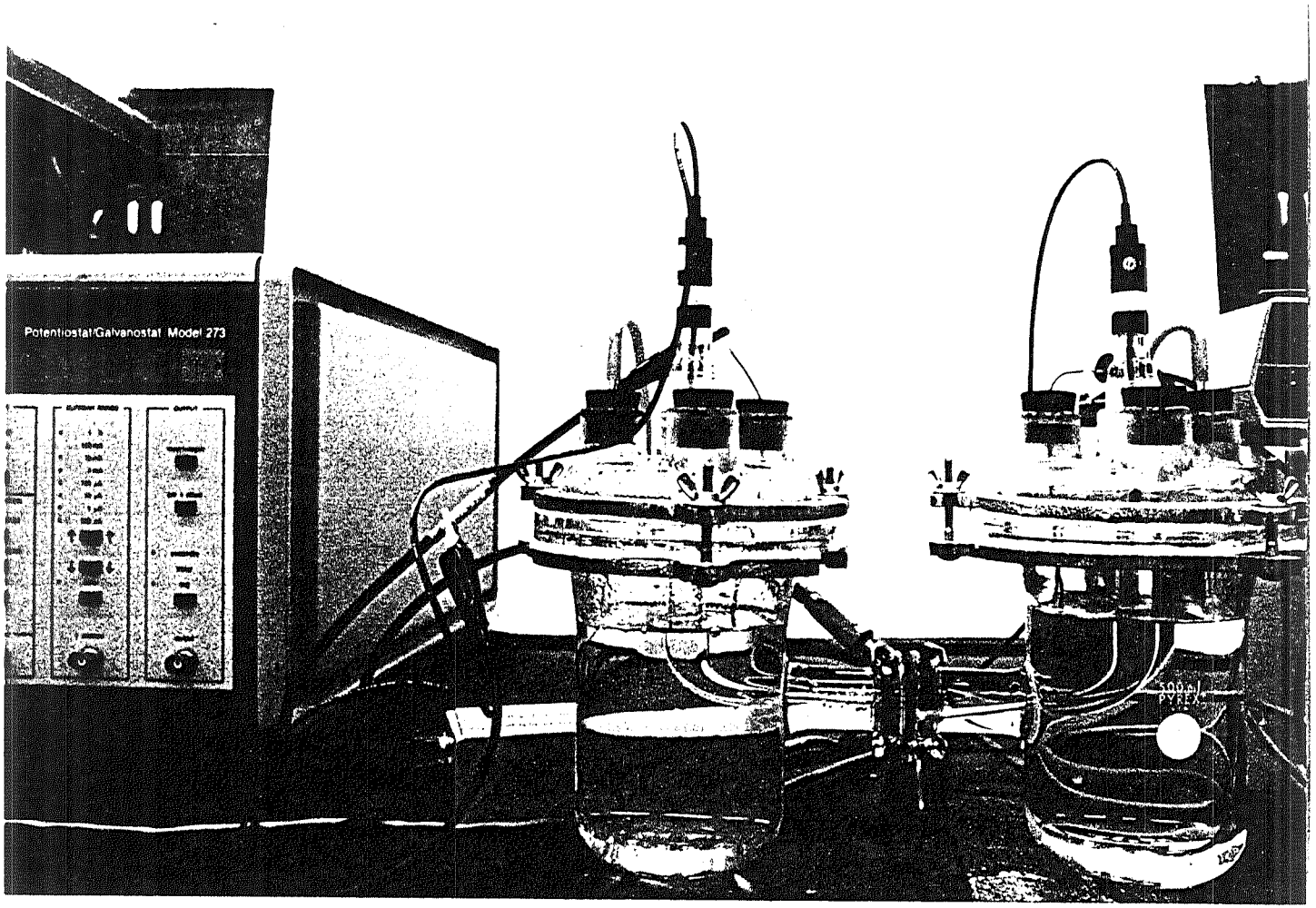

Figure 11 Experimental setup for H permeation studies

ORIGINAL PAGE IS
OF POOR QUALITY

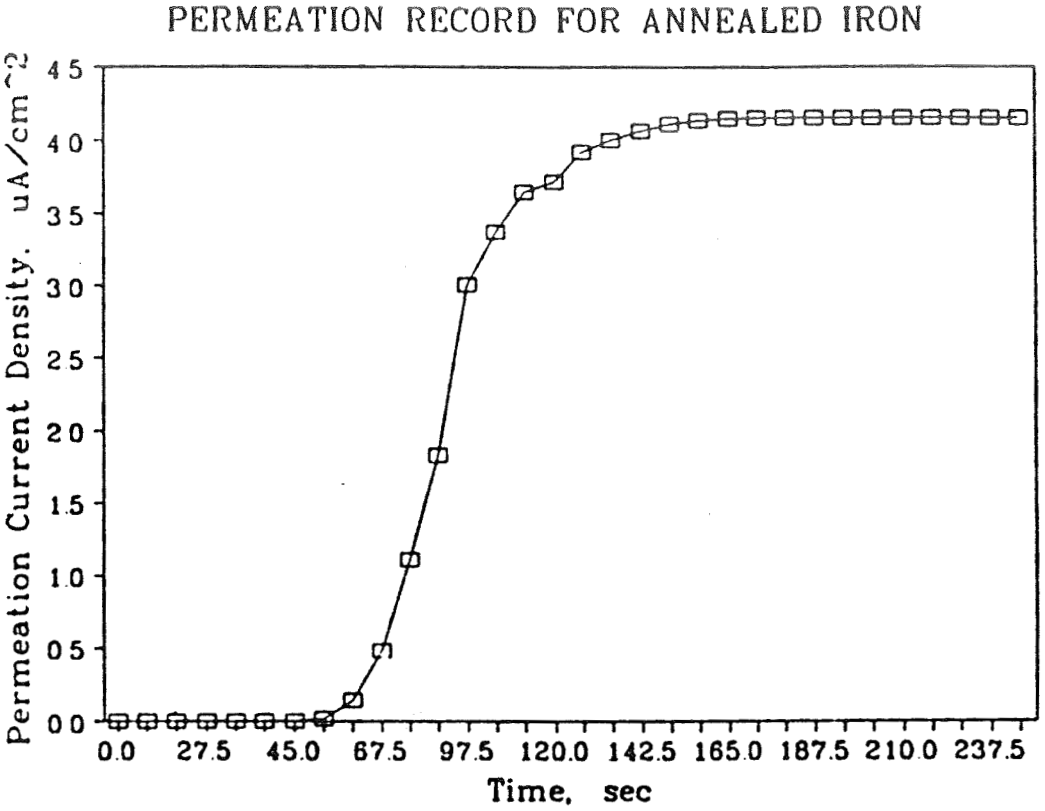

Figure 12

Results of Permeation on Annealed Iron

Diffusion Coefficient by Lag Time Calculation

9.94×10^{-7} cm²/s

Diffusion Coefficient by Breakthrough Calculation

7.93×10^{-7} cm²/s

Diffusion Coefficient by Rise Time Calculation

2.37×10^{-6} cm²/s

Table IV

3. Problems encountered in the experimental setup as reported in the quarterly presentations have been satisfactorily corrected.

4. With regards to embrittlement studies, Inconel 625 specimen has been tested in air by slow strain rate pulling at 10^{-6} per second. Another specimen of the same material is being cathodically charged by hydrogen before performing SSR tests.

5. Preliminary SEM and SAM fractographic studies have been performed to assess the impurity segregation to grain boundaries.

6. This research is being coordinated with White Sands Lab who will use hydrogen gas pressure to rupture the specimen discs and assess embrittlement.